12th Brazilian Congress of Manufacturing Engineering
May 10th-12th, 2023, Brasilia, DF, Brazil

THERMOMECHANICAL EVALUATION OF THERMOPLASTICS INJECTION CYCLE EFFECTS IN ALUMINIUM MOULDS USING THE FINITE ELEMENT METHOD

Gimaézio Gomes Carvalho
Márcio André Fernandes Martins
Armando Sá Ribeiro Junior
Universidade Federal da Bahia, R. Prof. Aristídes Novis, 2 - Federação, Salvador - BA, 40210-630, Brazil
gimaezio@hotmail.com; asrj@ufba.br; marciomartins@ufba.br

Gabriel Vasconcellos Bayma
Instituto Euvaldo Lodi – Ford Motor Company, Rua Edístio Pondé, SEDE, 342 – Stiep, Salvador – BA, 41770-395, Brazil
gvbayma@uol.com.br

Cristiano Vasconcellos Ferreira
Universidade Federal de Santa Catarina, Campus Universitário, s/n - Trindade, Florianópolis - SC, 88010-970, Brazil
cristiano.v.ferreira@ufsc.br

Valter Estevão Beal
SENAI CIMATEC, Av. Orlando Gomes, 1845 - Piatã, Salvador - BA, 41650-010, Brazil
valtereb@fieb.org.br

Abstract. *In the injection moulding process, it is important to mind the mould's lifespan, productivity as well as the moulded part quality. The mould stiffness is the most influential parameter during the packing stage, therefore predicting the mould mechanical behaviour when submitted to the loading cycles of the injection process is essential to the tooling project. Some loading sources are more likely to damage the tooling, such as the holding pressure, the clamping force, and the thermal stress. Also, it is important to consider the mould thermal cycle, evaluating heat exchange by conduction between the part and the mould, the free convection with the surrounding air and the forced convection with the cooling fluid. On the other hand, a poor mould mechanical project as well as the mould cooling system can result in bad quality moulded parts, long injection cycle or tooling damage. Moreover, steel mould's projects are well established while aluminium moulds are hardly ever cited in literature. The aluminium's thermal and mechanical properties are significantly different than steel ones, which change the injection cycle and its capability to resist the injection load cycles. This justifies the need to evaluate the differences in the use of both steel and aluminium materials in the mould design. This paper proposes numerical simulations making use of finite element method to assess the effects of the injection moulding loads on aluminium moulds, through outputs such as temperature profile, the stress state, and parting line openings. The results are compared to numerical results obtained for steel moulds. The results show that the difference between the mould's materials properties significantly changes the injection moulding conditions and the mould design, particularly the cooling system efficiency. These aspects are fundamental to make guidance to required modifications on the aluminium moulds, allowing the mould mechanical project and cooling system optimization to perform the best in terms of the part quality and process productivity.*

Keywords: *aluminium moulds; thermomechanical analysis; finite element method.*

1. INTRODUCTION

It is remarkable the number of industrial sectors that use thermoplastics as raw material for making geometrically complex products, from the injection moulding process (Farooque *et al*., 2020). Therefore, it is necessary to constantly produce technical data about this process, highlighting in this work those referring to the mould's resilience and performance.

Considering this scenario, it is also worth stating that for high-volume production, thermoplastic injection moulds are traditionally made of steel due to its good thermal stability and high mechanical strength. Nonetheless, despite these advantages, steel has a low thermal conductivity when compared to other metals, such as aluminium, which results in long injection cycles, mainly due to the longer time required to cool the part before demoulding.

Arieta Filho (2006) presents thermal and mechanical properties of four materials that are commonly used in thermoplastic injection moulds. Based on those data, it is possible to affirm that aluminium has a thermal conductivity about four times greater than steel. However, what hampers the use of this material in the mould manufacturing is its low

mechanical strength, when compared to steel, causing suspicion about its lifespan, which is measured by the number of parts that can be injected using these moulds.

These mechanical properties discouraged the use of aluminium moulds, which resulted in little information available in the literature on the various aspects related to the use of this type of tool. Nevertheless, the thermal properties suggest a significant gain in the injection cycle, and the aluminium alloys of the 7XXX series have the sufficient mechanical strength to withstand the injection pressures of thermoplastics (Arieta Filho, 2006).

Heat transfer within the mould is a complex transient three-dimensional problem. When starting the production, about 10 to 20 cycles are necessary to establish a steady-state regime, at which point the mould temperature evolution is the same for successive cycles (Sardo *et al*., 2019). During the injection moulding process, the moulds are submitted to three major loads: thermal stress due to heat transfer; stresses due to injection pressure imbalance; and the clamping force induced stress. In general, the thermoplastic injection moulding cycle consists of the following stages: mould closing; filling; packing; cooling; mould opening; and part ejection. Some of these steps are not relevant to be evaluated in terms of ensuring the mould design withstands the clamping force and the cavity pressure, for example, mould closing/opening and part ejection.

Chen *et al*. (2003) investigated the influence of processing parameters (including injection speed, melt temperature, mould temperature, filling–packing switchover and packing pressure) on the mould separation under different clamping forces. The associated variations of part weight were also measured. A simplified three-dimensional finite element model of mould structure on the core side plate was used for structural analysis. As there are interfaces, either between the mould and the part or between the mould itself, the thermal conductance becomes important in a simulation to better describe the heat transfer through these regions (Zhou *et al*., 2022). On the other hand, monitoring this property involves a complex and error-sensitive experimental procedure (Sardo *et al*., 2019). Somé *et al*. (2015) showed that the thermal conductance relies on the roughness of the mould and the polymer. Experiments revealed different thermal conductance values for a polypropylene-steel interface, considering several surface roughness and pressures. These data are applied in this work.

The main difference between this study and those are found in the literature is the thermomechanical evaluation of using aluminium in complex injection moulds. This paper considers a full three-dimensional mould model, in order to assess items like temperature profile, stress state and parting line openings. The authors are unaware of a work that modelled all these details through the finite element method, e.g., main components are fully modelled, forced convection in the cooling channels, natural convection with the surrounding air, thermal conductance in the interfaces.

2. METHODOLOGY

This paper proposes to simulate successive end-to-end injection cycles until steady state has been reached, then evaluate the stress state and parting line openings. This procedure is necessary to ensure a more representative temperature profile and, consequently, an accurate thermal stress state. The total cooling time was set as a variable through transient numerical simulations to determine the influence of this parameter on mould stress state.

This methodology was established to aim at thermomechanical evaluations, through numerical simulations, regarding effects in injection moulds arising from processing parameters variation. Particularly, the case study is directed to using aluminium as the mould material, when used for high-volume production. Evaluations changing only the mould material to steel are made to obtain a direct comparison between the two materials.

2.1 Geometry

For this work, a four parts mould (cavity plate, cavity, core plate and core) plus the moulded part were considered. The mould was designed to have four cooling channels on the cavity side (cavity + cavity plate) and two cooling channels on the core side (core + core plate), being aligned through four guide pins. There are also two holes that represent temperature monitored locations. The mould dimensions are 190.2 mm / 246.0 mm / 346.0 mm. The moulded part thickness is around 2.0 mm and represents a vehicular cupholder. Figure 1 shows the components.

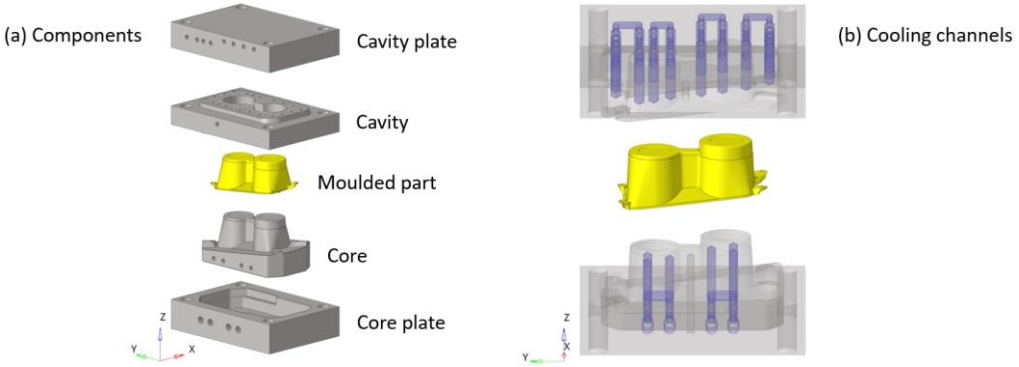

Figure 1. Mould and moulded part geometries

2.2 Numerical model

To evaluate the forces acting on the mould during the first injection cycle, the initial step is the transient heat transfer simulation up to end of the packing stage. At the beginning, uniform initial temperatures are established, both for the moulded part and the mould, with the thermomechanical simulation starting from a free strain state. The effect of plastic flow into the cavity during the filling stage is disregarded. The intermediate step of the simulation is a simultaneous application of clamping force and holding pressure, considering thermal strains from initial step. This step is performed through a static simulation. At the end of the intermediate step, both mould's stress state and the parting line openings are assessed. The final step consists of simulating the heat transfer until the mould opening. Boundary conditions must be properly imposed to faithfully represent what happens in the injection moulding machine. Gravity must be applied.

Heat transfer by conduction is the predominant phenomenon during the cooling, thus contact surfaces are used at the model interfaces to represent the solid-solid interaction, for both the thermal and mechanical purposes. Heat transfer by convection occurs simultaneously on the mould external surfaces – with the air – as well as in the cooling channels, so surfaces are defined for the adequate representation of this phenomenon. For the mechanical interaction, the friction coefficient is set, both for the polymer-mould interface and the mould's components interfaces. For the thermal interaction, suitable thermal conductance values are applied.

To simulate the second injection cycle, the same procedure is adopted, but assuming as an initial condition for the mould the final temperature profile of the previous cycle. For the moulded part, the application of a uniform initial temperature is kept, representing the end of the filling. This procedure is repeated for successive cycles until a stopping criterion that represents a steady state is met.

Upon completion of the planned numerical simulations, the temperature profile, stress state, and the parting line openings are verified to evaluate possible tooling damages or moulded part issues. This approach is schematically presented in Fig. 2.

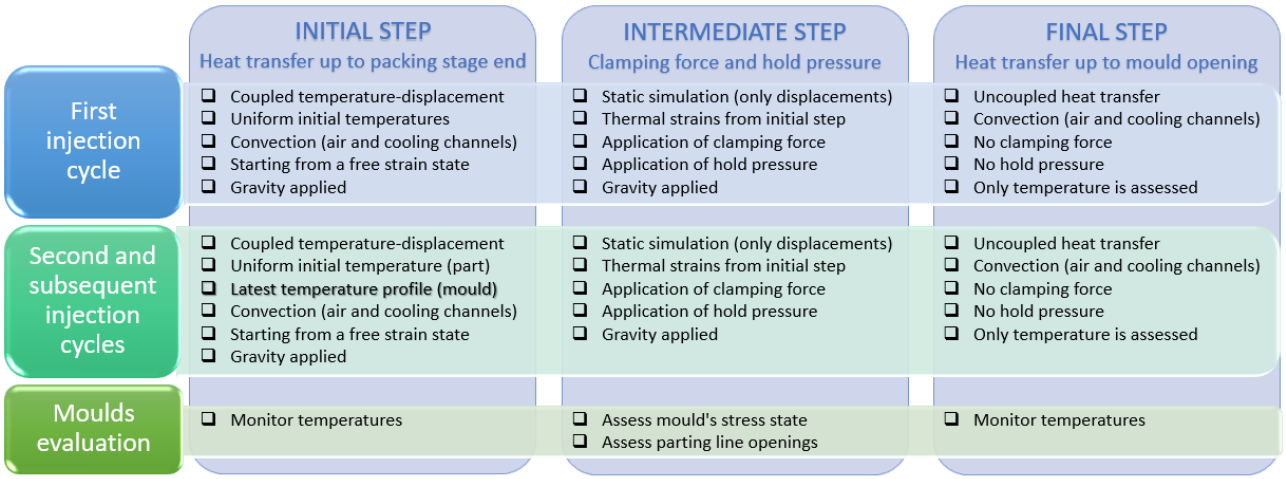

Figure 2. Approach to evaluate injection moulds through thermomechanical numerical simulations

A solver based on Finite Element Method (FEM) was used to run the coupled temperature-displacement, static, and uncoupled heat transfer simulations. It was built a mesh with 5684930 tetrahedral elements and 1107297 nodes. Table 1 shows the material properties that were applied in this work, both to the moulds and to the moulded part. These mechanical properties were obtained from the data sheet of the material suppliers.

Table 1. Steel, aluminium, and polypropylene properties

	Steel	Aluminium	Polypropylene (PP)
Density (kg/m³)	7890	2800	883
Poisson's ratio	0.30	0.34	0.38
Coefficient of thermal expansion (ºC^{-1})	0.000011	0.0000235	0.00015
Young's modulus (MPa)	210000	82116.6 at 82.22 ºC 79664.0 at 117.8 ºC 77609.0 at 160.9 ºC 75689.3 at 212.5 ºC	1700.0 at -40.0 ºC 1000.0 at 23.0 ºC 300.0 at 80.0 ºC 100.0 at 220.0 ºC
Specific heat [J/(kg · ºC)]	452	931.45	2800
Thermal conductivity [W/(m · ºC)]	48	136.87	0.15

In relation to the properties applied at the interfaces, the data were estimated by Somé *et al.* (2015). To estimate the film coefficient with the surrounding air, correlations for natural convection in external flows were used. To estimate the film coefficient with the cooling fluid (water), correlations for forced convection in internal flows were used. For this last one, a Moldex3D® preliminary simulation was necessary to estimate the Reynolds number. Table 2 shows the properties applied at the interfaces as well as the film coefficients.

Table 2. Properties applied to the interfaces and the film coefficients

	Polymer-mould interface	Mould-mould interface	Surrounding air	Cooling fluid (water)
Friction coefficient	0.4	0.1	-	-
Thermal conductance [W/(m^2 · ºC)]	4000.0 (0.0 mm) 1500.0 (1.0 mm) 0.0 (> 1.0 mm)	4000.0 (0.0 mm) 1500.0 (1.0 mm) 0.0 (> 1.0 mm)	-	-
Film coefficient [W/(m^2 · ºC)]	-	-	6.5	11433

2.3 Evaluation of the processing parameters contributions

As Huang *et al*. (2018) described, the clamping force can be estimated by multiplying the projected mould cavity area and the injection pressure. To verify the influence of these parameters in the tooling stress state and parting line separation, a set of processing parameters derived from Moldex3D® successful rheological simulations is used, as shown in Tab. 3.

Table 3. Processing parameters used initially in the simulations

Melt temperature	Initial mould temperature	Holding time	Holding pressure	Clamping force	Cooling time	Total time
220 ºC	20 ºC	6 s to 10 s	From rheological simulations	650 kN	12 s to 16 s	18 s to 26 s

The pressure profile that is applied to cavity elements was also obtained from Moldex3D® rheological simulation. The pressure ranges from 30 MPa (gate) to 24.3 MPa (point away from the gate), as shown in Fig. 3.

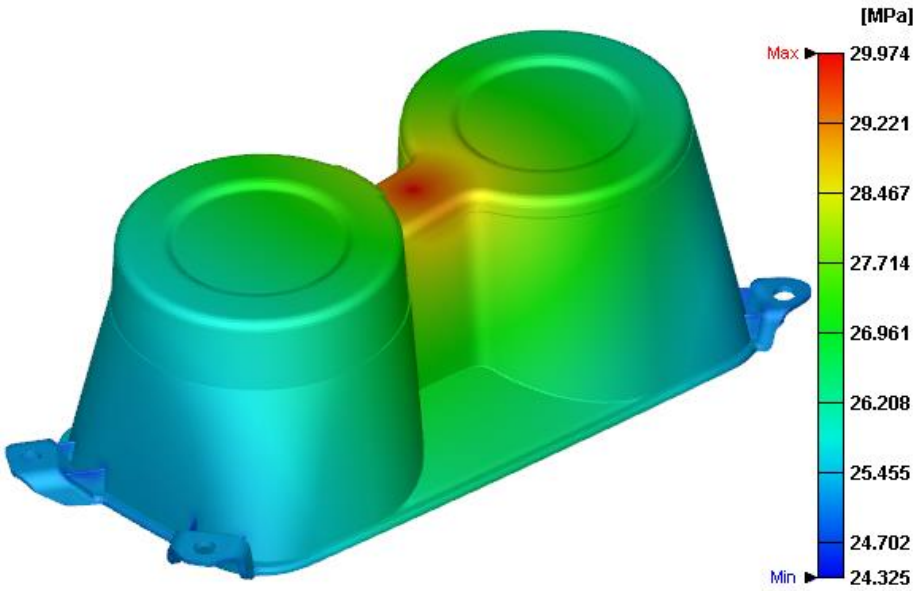

Figure 3. Maximum pressures verified from Moldex3D® rheological simulation

Hereby, it was set an evaluation plan to better understand how significant the cooling is on the temperature profile, stress state and mould parting line opening. The cooling time and the holding time are permuted using 12 s, 14 s and 16 s for cooling plus 6 s, 8 s and 10 s for holding. Therefore, the total time is the sum of holding time and cooling time. The filling stage is being disregarded in this work.

3. RESULTS

This section contains the results to aluminium and steel mould simulation, such as the temperature profile, stress state, and parting line openings.

3.1 Temperature profile

Three temperature histories were recorded, named locations A (core side) and B (cavity side), in addition to the average temperature of the moulded part, as shown in Fig. 4. The average temperature is the sum of all temperatures divided by the number of part nodes. The temperature results for both moulds are presented as a function of time and different cooling conditions.

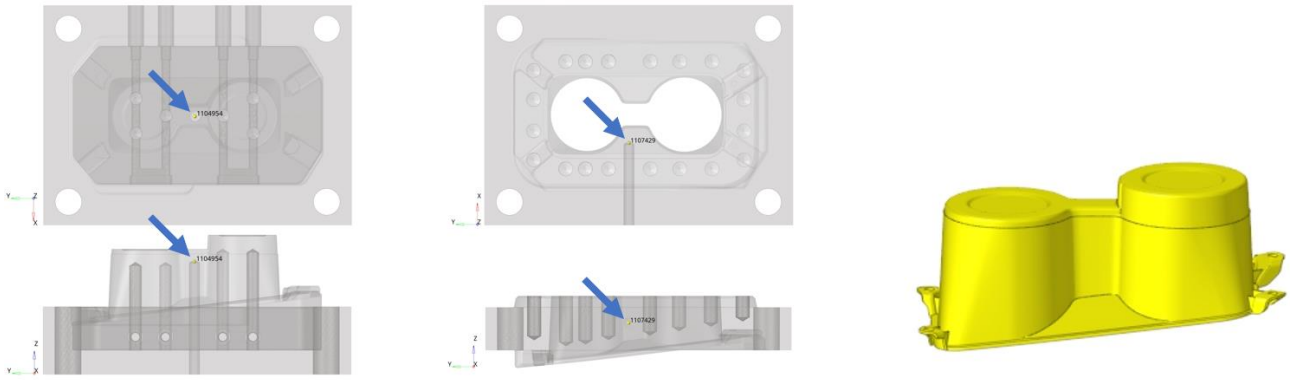

Figure 4. Node positions where temperature histories were recorded

Figure 5 shows temperature response comparisons between steel and aluminium moulds for a holding time of 6 s and cooling time of 12 s, totalling 18 s per cycle. Based on the results of the mould internal points and the part average temperature, it can be stated that the cyclic steady state in the steel mould occurs with a greater number of cycles (seven cycles) compared to the aluminium mould (four cycles), reaching higher temperature values but with a smaller thermal amplitude during cycles. When analysing the other cases, this pattern was also observed.

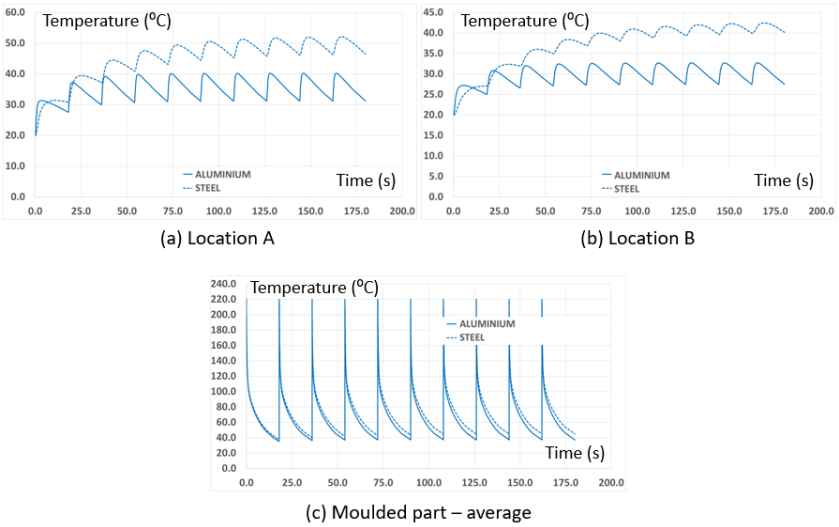

Figure 5. Temperature responses for a total time of 18 seconds per cycle

Additionally, analysing the moulded part hottest node during the 10th cycle for a total time of 18 s per cycle, it was observed that for both materials the hotspot final temperatures are very similar, as it was also verified in the rheological simulations. In the case of Polypropylene components, the hottest regions of the product reach about 100 ºC when the part is ejected, as mentioned by Ahuett-Garza *et al.* (2010). Therefore, the ejection temperature threshold was stablished at 100 ºC. Figure 6 shows the hottest node temperature responses during the 10th cycle for both materials. It is noticed that for the shortest total time (18 seconds), the moulded part can be ejected from both moulds, being approximately 16 s for aluminium mould and 17 s for steel mould. The reason why this point is almost equal in both moulds is because the hot spot is a region that cools considerably slower than others, due to its heat concentration.

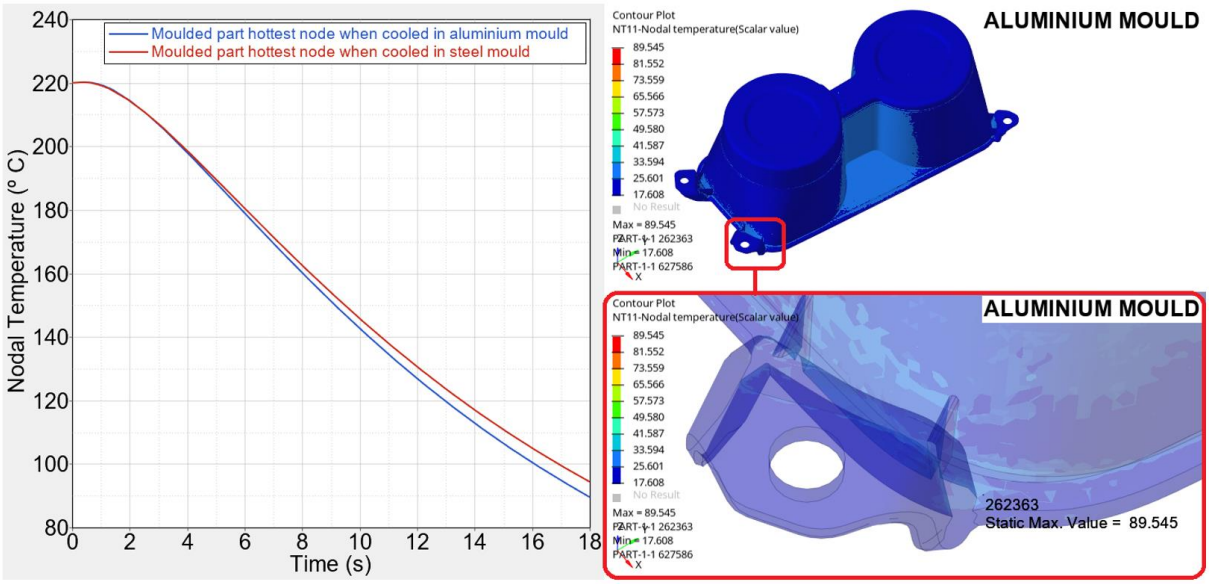

Figure 6. Moulded part hottest node during the 10th cycle for a total time of 18 seconds per cycle

Figure 7 shows the maximum temperature reached during 10th cycle at points A and B as a function of total time. As would be expected, for longer injection cycles the maximum temperature is lower than for faster injection cycles, with steel reaching higher temperatures than aluminium. The longer the injection cycle is, the closer the moulds' temperatures get.

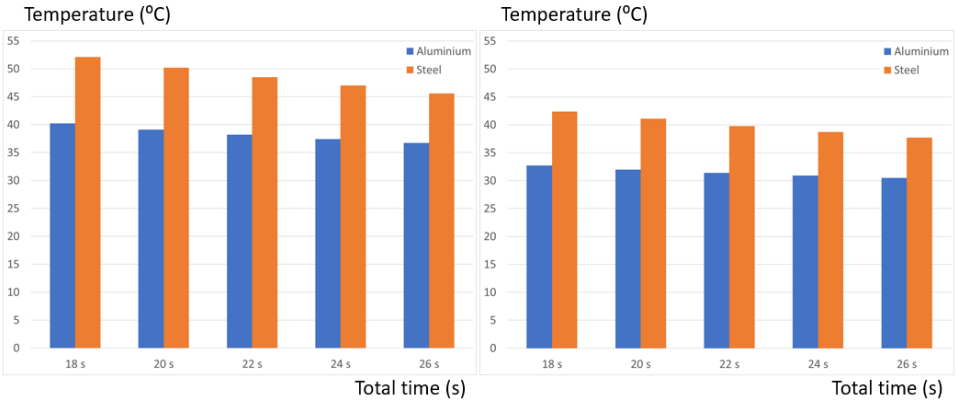

Figure 7. Maximum temperature responses as a function of total time

Figure 8 shows the temperatures at the ejection time of the 10th cycle. Based on these data, the moulded part average temperature when cooled in the aluminium mould for a period of 18 s is the same as the part cooled in a steel mould for 24 s, which proves the thermal efficiency of aluminium compared to steel tooling.

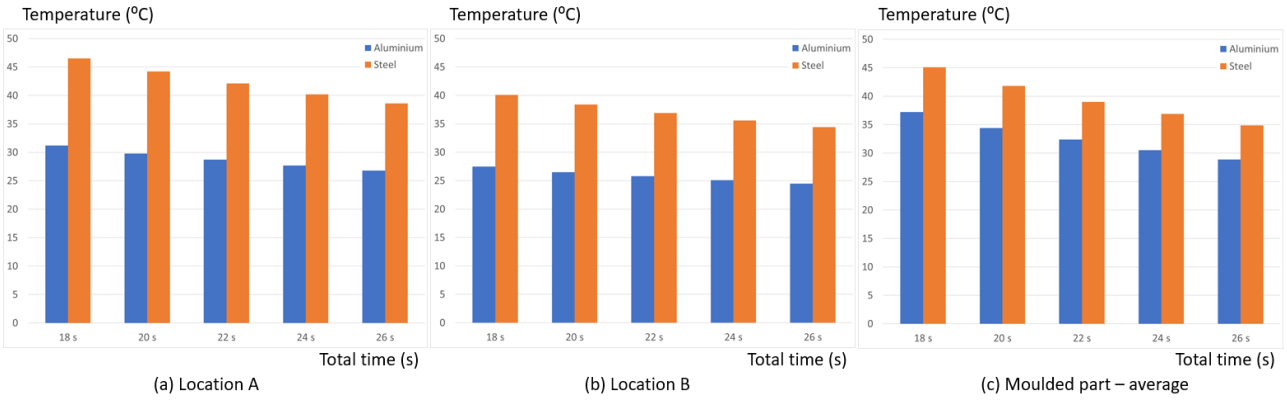

Figure 8. Temperatures responses at the ejection time as a function of total time

3.2 Stress state

Figure 9 presents the stress numerical results for both moulds. These data show the maximum principal and shear stresses acting on the mould during the packing stage at the cyclic steady state, which is due to temperature gradient, clamping force and holding pressure. The stress states observed are slightly greater for aluminium mould than for steel mould and becomes greater with the holding time increasing and lesser with the cooling time increasing.

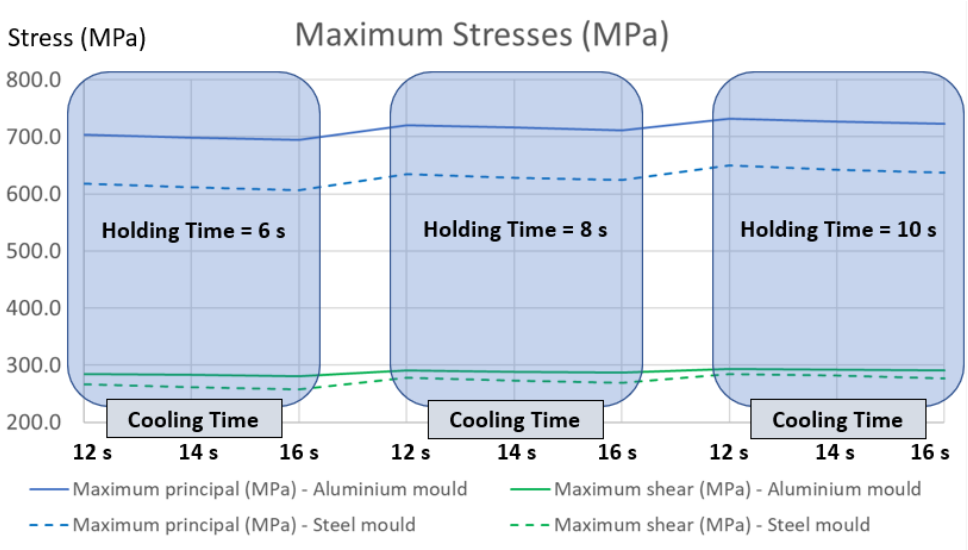

Figure 9. Stresses acting on the moulds during steady-state regime

Additionally, to understand how the stress state behaves during the transient regime, maximum stresses were collected for a holding time of 8 s and cooling time of 14 s, totalling 22 s per cycle, as shown in Fig. 10. The observed stresses are greater for the steady state than for the first cycle. The stresses are greater for aluminium mould than for steel mould.

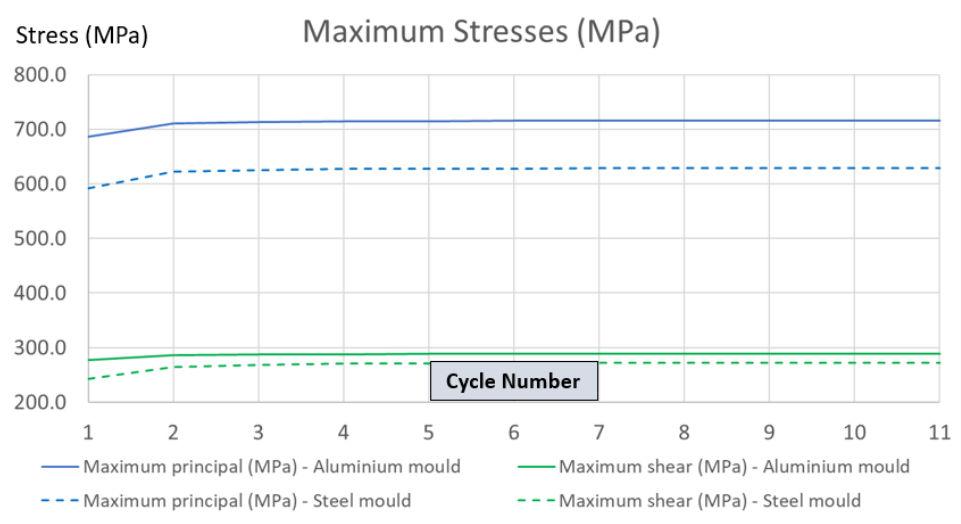

Figure 10. Stresses acting on the moulds during transient regime for a holding time of 8 s and cooling time of 14 s

As shown by Arieta Filho (2006), P20 steel usually has a yield strength of around 800 MPa. The failure criterion adopted for steel was von Mises (Distortion Energy Theory). The maximum von Mises stress monitored in steel mould was 531.9 MPa, below the yield strength. Aluminium alloy 7075 has a yield strength of about 500 MPa and the failure criterion adopted was Tresca (Maximum Shear Stress Theory). Thus, the target to be compared to the Maximum Shear Stress found (293.8 MPa) in aluminium mould is 250 MPa. Based on these results, the aluminium mould is susceptible to permanent deformations and the steel one is not, and changes in processing parameters or in the mould design are recommended so that aluminium benefits from its thermal advantages without harming the thermoplastic part manufacturing. Figure 11 shows the two elements where the maximum stresses were recorded. They belong to the component Cavity, as defined in Fig. 1.

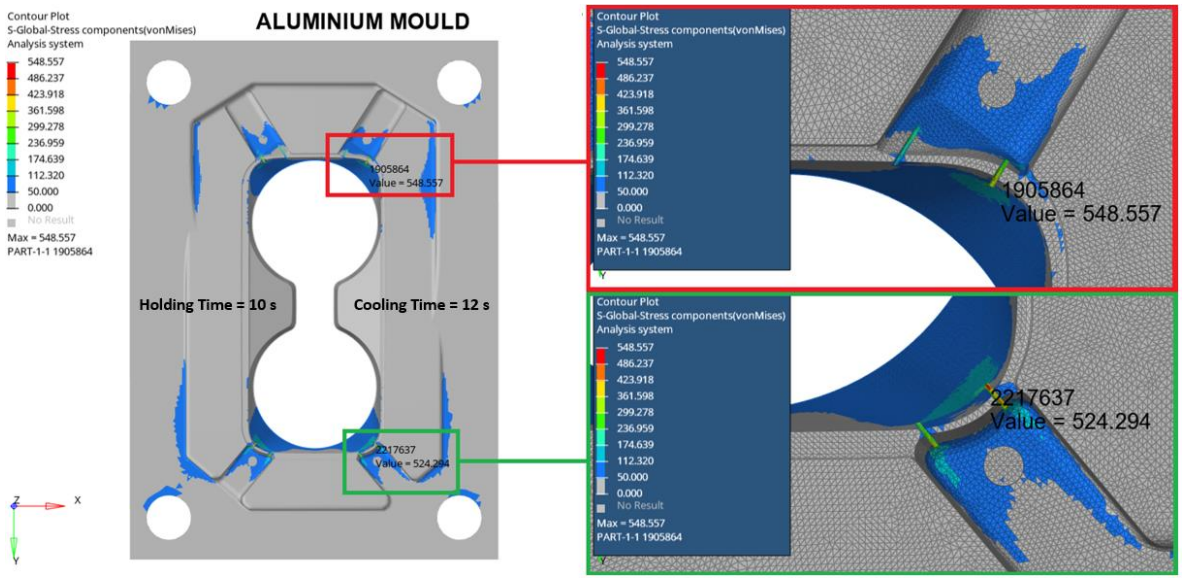

Figure 11. Mould area where the maximum stresses were recorded

Three simulations were devised to better understand the influence of each loading conditions: clamping force (C), holding pressure (P), and thermal loading (T). Initially, a static simulation was performed, considering only the clamping force of 650 kN. Subsequently, a new simulation was run considering the clamping force of 650 kN plus the holding pressure (C + P). Finally, the whole coupled temperature-displacement analysis was performed (C+P+T) during the cyclic steady-state regime. The holding time of 8 s and cooling time of 14 s were considered for this detailed investigation. As may be noticed from Fig. 12, the loading condition that increases the stresses of the two critical elements (ID 1905864 and ID 2217637), significantly, is the holding pressure.

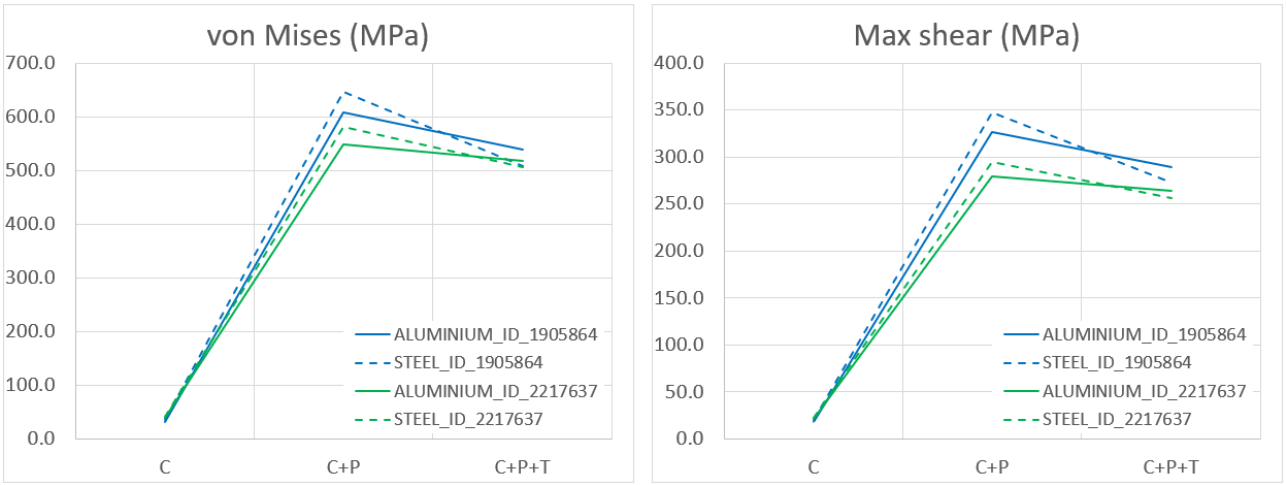

Figure 12. Loading condition breakdown and stresses evaluation for a holding time of 8 s and cooling time of 14 s

To evaluate in detail the loading condition contributions, the normal and shear stresses of the worst element (ID 1905864) were collected when cooled into both moulds. Then it was calculated the principal stresses, maximum shear stresses, and von Mises stresses, as shown in Tab. 4. Isolating the normal and shear stresses exclusively relating to holding pressure (P), it was observed that the maximum shear stress is greater than ones due to clamping force (C) or thermal loading (T). This data highlights the necessity to redefine the processing parameters in order to find lesser holding pressure values, which guarantee the quality of the moulded part. As it is a region responsible for the part conformation, mould design changes would also lead to a change in the part design. An important observation about this element is that it is undergoing positive normal stresses, even when only the stresses due to the holding pressure are considered. The animation of the C+P+T simulation was revised, confirming the behaviour of this critical element.

The stresses have exceeded the proportional limit in aluminium mould are unreal as the simulations do not consider elastic-plastic behaviour. The simulations only consider the linear mechanical properties of the materials, as shown in Tab. 1.

Table 4. Detailed stresses data of the critical mould element

Description	Element ID = 1905864									
	Aluminium Mould Stresses (MPa)					Steel Mould Stresses (MPa)				
	C	P	T	C+P	C+P+T	C	P	T	C+P	C+P+T
Normal Stress XX (from solver)	-21.2	754.9	-76.5	733.6	657.2	-26.1	744.0	-154.1	717.9	563.8
Normal Stress YY (from solver)	-7.4	263.8	-29.2	256.5	227.2	-7.2	208.9	-48.2	201.8	153.6
Normal Stress ZZ (from solver)	-10.6	242.4	-34.1	231.8	197.7	-9.9	189.3	-50.7	179.4	128.7
Shear Stress XY (from solver)	8.7	144.7	-35.4	153.4	117.9	6.6	152.2	-49.1	158.8	109.7
Shear Stress YZ (from solver)	0.0	17.4	-5.5	17.4	11.9	-0.4	20.9	-7.5	20.5	13.0
Shear Stress ZX (from solver)	14.0	-151.7	9.6	-137.8	-128.2	16.8	-159.6	24.1	-142.7	-118.6
von Mises Stress (from solver)	31.1	-	-	607.0	538.4	36.0	-	-	645.4	507.9
Max Shear Stress (from solver)	17.5	-	-	327.0	288.6	19.9	-	-	347.5	272.3
Principal stress - 1 (σ1)	2.1	828.8	-7.0	807.0	715.8	1.9	819.8	-20.1	791.5	617.1
Principal stress - 2 (σ2)	-8.3	272.0	-36.8	261.9	227.7	-7.2	221.0	-56.4	211.1	156.4
Principal stress - 3 (σ3)	-32.9	160.3	-96.0	153.0	138.5	-37.8	101.4	-176.5	96.5	72.5
Max shear stress (τmax)	17.5	334.3	44.5	327.0	288.6	19.9	359.2	78.2	347.5	272.3
Von Mises stress (σv)	31.1	620.4	78.5	607.0	538.4	36.0	666.6	141.8	645.4	507.9

3.3 Parting line openings

Huang *et al*. (2018) state that mould separation is often tolerated with an acceptable range (e.g., 0.075 mm) without causing flash. Therefore, as the cavity must not separate from the core more than 0.075 mm, it was observed that the aluminium mould tends to open more than the steel one, regardless the cooling condition. The maximum opening of the steel mould is 0.032 mm, while for the aluminium mould is 0.079 mm. Figure 13 shows the area where the maximum parting line openings were recorded, measured between the Cavity and the Core. Based on these results, solutions that aim to increase the aluminium moulds stiffness are necessary.

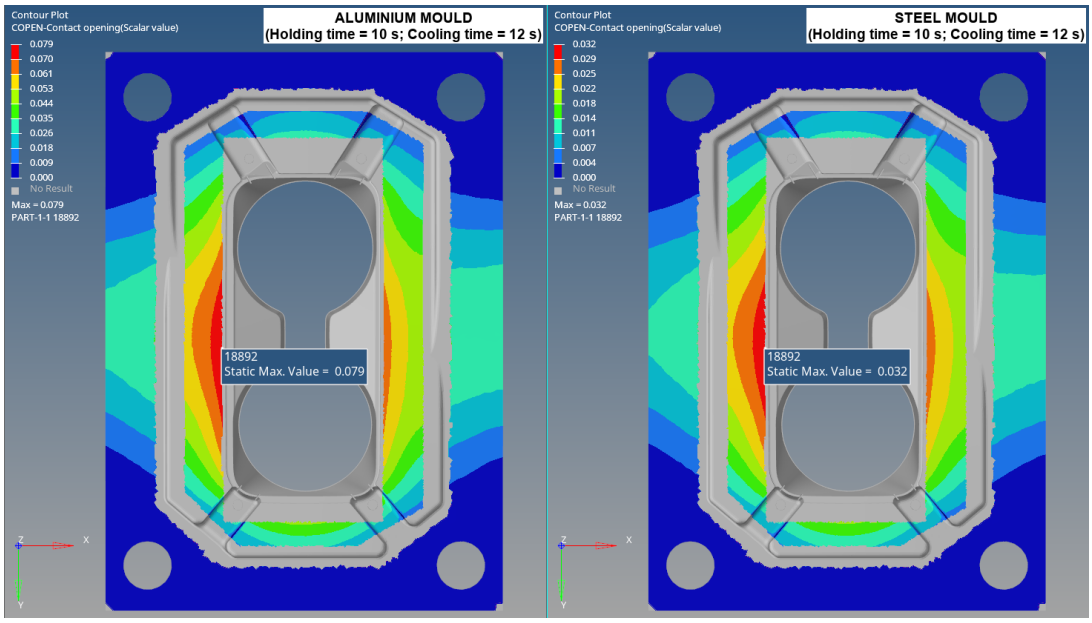

Figure 13. Parting line opening during steady-state regime of a holding time of 10 s and cooling time of 12 s

4. CONCLUSIONS

In this work, it was used a procedure based on finite elements to evaluate the temperature profile, the stress state and parting line openings in aluminium tooling, during the injection moulding process. The results were then compared with steel mould under the same operating conditions, which showed that the steady state in the steel mould occurs with a greater number of cycles, reaching higher temperature values than aluminium, but with lower thermal amplitude during the cycles. The maximum temperature is lower for longer injection cycles than for faster ones, with steel reaching higher temperatures than aluminium. The results show that the longer the injection cycle is, the closer the temperature profile of both moulds gets. It was noted that the average temperature of the moulded part when cooled in the aluminium mould for a period of 18 s is the same as the one cooled in a steel mould for 24 s, which proves the aluminium thermal efficiency compared to steel tooling. However, the time to reach the ejection, stablished by the temperature of the hot spot, is slightly

different. To solve this issue, solutions involving cooling systems must be considered and it was not objective of this work.

Regarding the numerical stress results, it was collected for both moulds the maximum von Mises (failure criteria for steel mould) and shear (failure criteria for aluminium mould) stresses acting on the mould during the packing stage of the cyclic steady state regime, which is due to the temperature gradient, clamping force and holding pressure. The stress states observed are slightly greater for aluminium mould than for steel mould and becomes greater with the holding time increasing and lesser with the cooling time increasing. Additionally, to understand how the stress state behaves during the transient regime, maximum stresses were collected from all cycles of a specific case, and it was observed that stresses are greater for the steady state than for the first cycle.

The aluminium mould is susceptible to permanent deformations that steel is not, and changes in processing parameters or mould design are recommended so that aluminium benefits from its thermal advantages without harming the thermoplastic part manufacturing. The contribution of each loading was calculated, and the stresses caused by holding pressure were the greatest. The thermal loading relieved the stress state caused by clamping force and holding pressure. In addition, both the thermal loading and the clamping force decrease the stress state due to the holding pressure.

In relation to parting line openings, as the cavity must not separate from the core more than 0.075 mm to avoid flash, it was observed that the aluminium mould tends to open more than the steel one, regardless the cooling condition. The maximum opening for the steel mould is 0.032 mm, while for the aluminium mould is 0.079 mm. Based on these results, solutions that aim to increase the aluminium moulds stiffness are necessary.

Imperatively for this vehicular cupholder mould, the aluminium mould must be reinforced to reduce the parting line openings, and it is also important to use minimum holding pressure to minimize stresses. Therefore, the results showed that the difference between the mould's materials properties significantly changes the injection moulding conditions and the mould design, particularly the cooling system efficiency. These aspects are fundamental to make guidance to required modifications on the aluminium moulds, allowing the mould mechanical project and cooling system optimization to perform the best in terms of the part quality and process productivity. For future works, it is suggested to study different mould designs and different parameters combinations.

5. ACKNOWLEDGEMENTS

This work is a partial result from the Project DEMALAP - Demonstrador de Molde em Alumínio para Alta Produção (High production aluminum mold demonstrator) sponsored by Programa Rota 2030 from Brazilian Government described in Federal Law No. 13.755/2018 and it is coordinated by FUNDEP. The executors of this project are the universities SENAI CIMATEC, UFBA and UFSC. We thank the other partners of the project for their support: ESSS Engineering Simulation and Scientific Software Ltda.; Ford Motor Company Brasil Ltda., Moldit Brasil Ltda.; Open Mind Tecnologia Brasil Ltda.; Renault do Brasil S.A.; SMRC Fabricação e Comércio de Produtos Automotivos do Brasil Ltda. e Union Indústria de Moldes e Comércio Atacadista de Máquinas Eireli.

6. REFERENCES

Ahuett-Garza, H., Aguiar, F. and Ponce, V. 2010. Modeling and analysis of post ejection wall deflections in products made out of polypropylene. *Polymer Engineering and Science 50(5), pp. 1007-1018.*

Arieta Filho, F.G. 2006. Ligas de alumínio de alta resistência para moldes de injeção de termoplásticos: ficção ou realidade? Revista Ferramental. Brazilian magazine of the tooling industry. Edition 8. Pages 37 - 44. 19 Aug. 2022 <https://issuu.com/revistaferramental8/docs/edi____o_8>.

Chen, S.-C., Liaw, W.-L., Su, P.-L. and Chung, M.-H. 2003. Investigation of Mold Plate Separation in Thin-wall Injection Molding. *Advances in Polymer Technology 22(4), pp. 306-319.*

Farooque, R., Asjad, M. and Rizvi, S.J.A. 2020. A current state of art applied to injection moulding manufacturing process - A review. *Materials Today: Proceedings 43, pp. 441-446.*

Huang, M.-S., Nian, S.-C., Chen, J.-Y. and Lin, C.-Y. 2018. Influence of clamping force on tie-bar elongation, mold separation, and part dimensions in injection molding. *Precision Engineering 51, pp. 647-658.*

Sardo, L., Daldoul, W., Vincent, M. and Toulorge, T. 2019. Simulations of Heat Transfer in Thermoplastic Injection Molds Manufactured by Additive Techniques. *International Polymer Processing, vol. 34, no. 1, pp. 37-46.*

Somé, S.C., Delaunay, D., Faraj, J., Bailleul, J.L., Boyard, N. and Quilliet, S. 2015. Modeling of the thermal contact resistance time evolution at polymer-mold interface during injection molding: Effect of polymers' solidification. *Applied Thermal Engineering 84, pp. 150-157.*

Zhou, T., Zhao, Y. and Rao, Z. 2022. Fundamental and estimation of thermal contact resistance between polymer matrix composites: A review. *International Journal of Heat and Mass Transfer 189, 122701.*

7. RESPONSIBILITY NOTICE

The authors are the only responsible for the printed material included in this paper.